



## **Arabidopsis STAY-GREEN2 is a negative regulator of chlorophyll degradation during leaf senescence**

Sakuraba, Yasuhito ; Park, So-Yon ; Kim, Ye-Sol ; Wang, Seung-Hyun ; Yoo, Soo-Cheul ;  
Hörtensteiner, Stefan ; Paek, Nam-Chon

**Abstract:** Chlorophyll (Chl) degradation causes leaf yellowing during senescence or under stress conditions. For Chl breakdown, STAY-GREEN1 (SGR1) interacts with Chl catabolic enzymes (CCEs) and light-harvesting complex II (LHCII) at the thylakoid membrane, possibly to allow metabolic channeling of potentially phototoxic Chl breakdown intermediates. Among these Chl catabolic components, SGR1 acts as a key regulator of leaf yellowing. In addition to SGR1 (At4g22920), the *Arabidopsis thaliana* genome contains an additional homolog, SGR2 (At4g11910), whose biological function remains elusive. Under senescence-inducing conditions, SGR2 expression is highly up-regulated, similarly to SGR1 expression. Here we show that SGR2 function counteracts SGR1 activity in leaf Chl degradation; SGR2-overexpressing plants stayed green and the *sgr2-1* knockout mutant exhibited early leaf yellowing under age-, dark-, and stress-induced senescence conditions. Like SGR1, SGR2 interacted with LHCII but, in contrast to SGR1, SGR2 interactions with CCEs were very limited. Furthermore, SGR1 and SGR2 formed homo- or heterodimers, strongly suggesting a role for SGR2 in negatively regulating Chl degradation by possibly interfering with the proposed CCE-recruiting function of SGR1. Our data indicate an antagonistic evolution of the functions of SGR1 and SGR2 in *Arabidopsis* to balance Chl catabolism in chloroplasts with the dismantling and remobilizing of other cellular components in senescing leaf cells.

DOI: <https://doi.org/10.1093/mp/ssu045>

Posted at the Zurich Open Repository and Archive, University of Zurich

ZORA URL: <https://doi.org/10.5167/uzh-104525>

Journal Article

Accepted Version

Originally published at:

Sakuraba, Yasuhito; Park, So-Yon; Kim, Ye-Sol; Wang, Seung-Hyun; Yoo, Soo-Cheul; Hörtensteiner, Stefan; Paek, Nam-Chon (2014). *Arabidopsis STAY-GREEN2 is a negative regulator of chlorophyll degradation during leaf senescence*. *Molecular Plant*, 7(8):1288-302.

DOI: <https://doi.org/10.1093/mp/ssu045>

**Title Page**

**Running title:** Negative Role of SGR2 in Chlorophyll Degradation

**Manuscript title:** *Arabidopsis* STAY-GREEN2 Is a Negative Regulator in Chlorophyll Degradation during Leaf Senescence

**Authors:**

Yasuhito Sakuraba<sup>a</sup>, So-Yon Park<sup>a,2</sup>, Ye-Sol Kim<sup>a,3</sup>, Soo-Cheul Yoo<sup>a,4</sup>, Seung-Hyun Wang<sup>a</sup>, Stefan Hörtensteiner<sup>b</sup>, and Nam-Chon Paek<sup>a,c,1</sup>

**Affiliations:**

**a** Department of Plant Science, Plant Genomics and Breeding Institute, and Research Institute for Agriculture and Life Sciences, Seoul National University, Seoul 151-921, Korea.

**b** Institute of Plant Biology, University of Zurich, CH-8008 Zurich, Switzerland.

**c** Institute of Green Bio Science and Technology, Seoul National University, Pyeongchang 232-916, Korea.

<sup>1</sup> To whom correspondence should be addressed. E-mail: ncpaek@snu.ac.kr, tel. +82 10 6324 2302, fax +82 2 877 4550.

<sup>2</sup> Present address: Division of Plant Sciences, University of Missouri, Columbia, MO 65211.

<sup>3</sup> Present address: Advanced Radiation Technology Institute, Korea Atomic Energy Research Institute, Jeongeup 580-185, Korea

<sup>4</sup> Present address: Department of Bioresource and Rural System of Engineering, Hankyong National University, Ansong 456-749, Korea

**Corresponding author:**

Nam-Chon Paek

Tel: +82 10 6324 2302

Fax: +82 2 877 4550

E-mail: ncpaek@snu.ac.kr

## ***Arabidopsis* STAY-GREEN2 Is a Negative Regulator in Chlorophyll Degradation during Leaf Senescence**

### **ABSTRACT**

Chlorophyll (Chl) degradation causes leaf yellowing during senescence or under stress conditions. For Chl breakdown, STAY-GREEN1 (SGR1) interacts with Chl catabolic enzymes (CCEs) and light-harvesting complex II (LHCII) at the thylakoid membrane, possibly to allow metabolic channeling of potentially phototoxic Chl breakdown intermediates. Among these Chl catabolic components, SGR1 acts as a key regulator for leaf yellowing. In addition to *SGR1* (At4g22920), the *Arabidopsis thaliana* genome contains an additional homolog, *SGR2* (At4g11910), whose biological function remains elusive. Under senescence-inducing conditions, *SGR2* expression is highly up-regulated, similar to *SGR1* expression. Here we show that SGR2 function counteracts SGR1 activity in leaf Chl degradation; *SGR2*-overexpressing plants stayed green and the *sgr2-1* knockout mutant exhibited early leaf yellowing under age-, dark-, and stress-induced senescence conditions. Like SGR1, SGR2 interacted with LHCII, but in contrast to SGR1, SGR2 interactions with CCEs were considerably limited. Furthermore, SGR1 and SGR2 formed homo- or heterodimers, strongly suggesting a role for SGR2 in negatively regulating Chl degradation by possibly interfering with the proposed CCE-recruiting function of SGR1. Our data indicate an antagonistic evolution of the functions of SGR1 and SGR2 in *Arabidopsis* to allow balancing of Chl catabolism in chloroplasts with dismantling and remobilizing processes of other cellular components in senescing leaf cells.

**Key words:** *Arabidopsis thaliana*; stay-green; *SGR1*; *SGR2*; chlorophyll degradation; leaf senescence; abiotic stress.

## INTRODUCTION

During senescence, plants recycle valuable nutrient components from leaves, to maximize viability in the next generation (Hörtensteiner and Feller, 2002; Lim et al., 2007). In senescence, among other degradation processes, chlorophyll (Chl) is converted to colorless breakdown products in a multi-step catabolic pathway. This pathway consists of several chloroplast-located reactions that require six known Chl catabolic enzymes (CCEs) and a metal-chelating substance (MCS) that remains to be identified (Hörtensteiner and Kräutler, 2011). All six CCEs have been characterized in *Arabidopsis thaliana*. The first part of breakdown is the two-step reduction of Chl *b* to Chl *a* by Chl *b* reductase (CBR) and 7-hydroxymethyl Chl reductase (HCAR) (Scheumann et al., 1998). Genes encoding two CBR isoforms, *NON-YELLOW COLORING1* (*NYC1*) and *NYC1-LIKE* (*NOL*), have been identified in rice (*Oryza sativa*) and *Arabidopsis* (Horie et al., 2009; Sato et al., 2009). During natural and dark-induced senescence, *Arabidopsis nyc1* and rice *nyc1* and *nol* mutants show stay-green phenotypes with dominant retention of Chl *b* and LHCII subunits (Kusaba et al., 2007; Sato et al., 2009; Horie et al., 2009). However in *Arabidopsis*, *nol* mutants do not show any phenotype, and *NOL* expression patterns differ considerably from *NYC1* (Horie et al., 2009; Sakuraba et al., 2013), suggesting that in *Arabidopsis*, these two CBR isoforms may have a similar function in Chl metabolism, but act at different developmental stages. *HCAR* has recently been identified in *Arabidopsis* (Meguro et al., 2011). Although *Arabidopsis hcar* mutants show a stay-green phenotype under dark-induced senescence, *HCAR* mRNA levels are the most abundant at early vegetative growth and leaf greening stages throughout development, similar to *NOL* expression (Sakuraba et al., 2013). Furthermore, *HCAR* strongly interacts with *NOL* in yeast two-hybrid assays, suggesting that the *HCAR-NOL* interaction may function in Chl turnover in presenescent leaves in *Arabidopsis*. The next step in the pathway is the removal of the central Mg atom of Chl *a* by MCS to yield a Mg-free Chl intermediate, pheophytin *a* (Phein *a*). Pheophytinase (PPH), catalyzing the hydrolysis of Phein *a* to produce pheophorbide *a* (Pheide *a*), was identified by bioinformatics in *Arabidopsis* and by map-based cloning of the stay-green *nyc3* mutant in rice (Schelbert et al., 2009; Morita et al., 2009). Subsequently, the chlorin macrocycle of Pheide *a* is oxygenolytically opened by Pheide *a* oxygenase (PAO) (Pružinská et al., 2003), and the product of this reaction, red Chl catabolite (RCC), is reduced to a non-phototoxic primary fluorescent Chl catabolite (pFCC) by RCC reductase (RCCR) (Pružinská et al., 2007). *PAO*- and *RCCR*-impaired mutants, originally identified as *accelerated cell death1* (*acd1*) and *acd2* mutants, respectively (Greenberg et al., 1994, 2002), exhibit severe leaf necrosis phenotypes that are caused by the accumulation of respective phototoxic Chl breakdown intermediates, i.e. Pheide *a* and RCC (Mach et al., 2001; Pružinská et al., 2007; Hirashima et al., 2009).

In addition to CCEs and MCS, *STAY-GREEN1* (*SGRI*) also acts as a key regulator of Chl degradation. Mutations in *SGRI* orthologs cause a stay-green phenotype in many plant species, such as *Arabidopsis* (e.g. *nonyellowing 1* [*nye1-1*]; Ren et al., 2007), rice (Park et al., 2007), pea (*Pisum*

*sativum*; Sato et al., 2007), tomato (*Solanum lycopersicum*; Barry et al., 2008) and bell pepper (*Capsicum annuum*; Barry et al., 2008), tall fescue (*Festuca arundinacea*; Wei et al., 2011), *Medicago truncatula* (Zhou et al., 2011), and soybean (Fang et al., 2014). SGR1 specifically interacts with light-harvesting complex subunits of photosystem II (LHCII), but not with other components of photosystem complexes, including core complex and LHCI subunits (Park et al., 2007; Sakuraba et al., 2012b). Furthermore, we recently found that SGR1 physically interacts with all six known CCEs (i.e. NOL, NYC1, HCAR, PPH, PAO and RCCR), and forms a multi-protein, possibly highly dynamic, complex for Chl detoxification during natural senescence (Sakuraba et al., 2012b; Sakuraba et al., 2013). Recently, an another *Arabidopsis* mutant in *SGR1*, *no chlorosis1 (noc1)*, was isolated by screening for plants that show altered disease symptoms after *Pseudomonas syringae* pv *tomato* (*Pst*) DC3000 infection (Mecey et al., 2011); *noc1* mutants stayed green for several days after bacterial infection, indicating that SGR1 is also involved in disease-induced leaf chlorosis.

Most higher plant species have two or more *SGR1* homologs, all of which are predicted to localize to the chloroplast (Park et al., 2007; Barry et al., 2008), strongly suggesting that they also function in plastids and possibly in Chl metabolism. However, in *M. truncatula* *SGR* is expressed during nodule senescence in roots (Zhou et al., 2011), indicating a possible Chl degradation-independent function. Phylogenetic analysis revealed that the SGR protein family of higher plants can be classified into two groups (Barry et al., 2008; Aubry et al., 2008; Hörtensteiner, 2009) (**Supplemental Figures 1 and 2**). One group, considered to be the genuine SGR subfamily, contains members for which mutations cause a stay-green phenotype (Ren et al., 2007; Park et al., 2007; Barry et al., 2008). The second SGR subfamily, termed SGR LIKE (SGRL), is distinct from the SGR subfamily, but contains highly conserved members from different plant species. It was recently reported that transgenic rice plants overexpressing rice *SGRL* exhibited early leaf yellowing during dark-induced senescence (Rong et al., 2013), strongly suggesting that SGRL has almost the same function as SGR1 in rice.

The *Arabidopsis* genome contains three *SGR* homologs, termed *SGR1/NYE1* (At4g22920), *SGR2* (At4g11910), and *SGRL* (At1g44000), similar to soybean (**Supplemental Figures 1 and 2**). To date, the molecular, physiological and biochemical functions of *Arabidopsis* SGR1/NYE1 have been well-characterized (Ren et al., 2007; Mur et al., 2010; Mecey et al., 2011; Sakuraba et al., 2012b). Like rice SGRL (Rong et al., 2013), it is possible that *Arabidopsis* SGRL also contributes to Chl breakdown or Chl turnover in presenescent leaves. Recently, it has been reported that the stay-green phenotype of the *d1d2* double mutant in soybean is caused by null mutations of both *D1/SGR1* and *D2/SGR2* (Fang et al., 2014), indicating that the two senescence-induced SGR proteins, D1 and D2, function redundantly to promote Chl breakdown during leaf senescence. In addition, Delmas et al. (2013) reported that *Arabidopsis* *SGR1* and *SGR2* expression is up-regulated by *ABA INSENSITIVE 3 (ABI3)* for embryo degreening during seed maturation. However, the *Arabidopsis* *sgr2-1* knockout mutant did not display the stay-green phenotype during leaf senescence (Aubry et al., 2008). Thus, the molecular,

physiological and biochemical functions of *Arabidopsis* SGR2 during Chl metabolism of senescing leaves remain ambiguous.

Here, we functionally analyzed *Arabidopsis* SGR2 under various senescence-inducing conditions. We show that SGR2-overexpressing (SGR2-OX) plants exhibit a stay-green phenotype, and *sgr2-1* knockout mutants show slightly earlier leaf yellowing during age- and dark-induced senescence. We also found that in contrast to accelerated leaf yellowing of SGR1-OX plants, SGR2-OX plants maintained leaf greenness much longer also under abiotic stress-induced senescence conditions, such as salinity, drought, high temperature and high light stresses. Similar to SGR1 biochemical function, SGR2 interacts with LHCII subunits at the thylakoid membranes *in vivo*. However, compared to SGR1, we found that the capacity of SGR2 to interact with CCEs was considerably limited. Furthermore, SGR1 and SGR2 formed homodimers or heterodimers, which may negatively affect the SGR1 interaction efficiency with CCEs, a prerequisite for initiation of Chl breakdown.

## RESULTS

### Expression of the Three SGR Homologs in *Arabidopsis*

Higher plants have two or more SGR homologs, and phylogenetic analysis indicates that they can be divided into two evolutionarily distinct subfamilies, i.e. SGR and SGR LIKE (SGRL) (**Supplemental Figure 1**; Barry et al., 2008). While two SGR homologs exist in rice (SGR and SGRL), *Arabidopsis* has three SGR homologs, termed SGR1/NYE1 (At4g22920), SGR2 (At4g11910) and SGRL (At1g44000).

We examined the expression patterns of the three *Arabidopsis* SGR homologs during plant development under long day (LD) and under dark-induced senescence conditions. Under long day conditions, expression of SGR1 and SGR2 was rapidly up-regulated during natural senescence (about 4 weeks after germination [WAG]) (**Figure 1A** and **1B**). By contrast, SGRL expression was up-regulated during early vegetative stages, peaked at 3 WAG, and decreased thereafter (**Figure 1C**). Similar expression patterns were observed during dark-induced senescence; SGR1 and SGR2 expression increased and peaked at 3 d of dark incubation (DDI) (**Figure 1D** and **1E**), while SGRL expression was rapidly down-regulated in darkness (**Figure 1F**). Based on the similar pattern of SGRL expression in rice (Rong et al., 2013) and *Arabidopsis*, it is highly possible that *Arabidopsis* SGRL is involved in Chl degradation or Chl turnover in presenescent leaves, similar to rice SGRL (Rong et al., 2013).

The structures of SGR1 and SGR2 are considerably similar; a conserved central domain, termed the SGR domain, separates the highly variable N-terminal (containing the predicted chloroplast transit peptide) and C-terminal regions (**Supplemental Figure 3**). However, a biochemical function for

SGR2 during leaf senescence remains ambiguous, because it was reported that the *sgr2-1* knockout mutant is not defective in Chl catabolism, unlike the *nye1-1* stay-green mutant (Ren et al., 2007; Aubry et al., 2008).

### **SGR2-Overexpressing Plants Stayed Green during Dark-Induced Senescence**

To find a possible physiological function of *SGR2*, we created the C-terminal TAP (Tandem Affinity Purification)-tagged overexpressing (OX) *Arabidopsis* plants for two *SGR* genes, termed *SGR1*-OX (as a control; Sakuraba et al., 2012b), and *SGR2*-OX (**Supplemental Table 1**). Expression levels of the *SGR* genes in these lines were examined by reverse transcription-quantitative real time PCR (RT-qPCR), and the lines showing the highest expression, *SGR1*-OX#4 and *SGR2*-OX#3, were selected for further studies (**Supplemental Figure 4**). None of these lines showed any obvious phenotype during vegetative stages under long day conditions (**Figure 2A**, 0 DDI). Remarkably, however, under dark-induced senescence conditions (**Figure 2A**, 8 DDI), *SGR2*-OX showed a strong stay-green phenotype that was opposite to the accelerated leaf yellowing of *SGR1*-OX, as reported previously (Mur et al., 2010; Sakuraba et al., 2012b). The stay-green phenotype of *SGR2*-OX was further confirmed in other independent transgenic lines (**Supplemental Figure 5**). During dark-induced senescence, levels of total Chl (**Figure 2B**) and photosystem subunits (**Figure 2C**) remained much higher in *SGR2*-OX leaves compared to wild-type leaves, but they declined faster in *SGR1*-OX leaves (as shown in Sakuraba et al., 2012b). The stay-green phenotype of *SGR2*-OX leaves was also observed during natural senescence (**Supplemental Figure 6**) as well as upon senescence induction in the presence of methyl jasmonate (MeJA) (**Supplemental Figure 7**).

Stay-green varieties have been divided into several subgroups and are categorized into functional (types A and B) and nonfunctional (types C, D and E) stay-greens (Thomas and Howarth, 2000; Hörtensteiner, 2009). It has been reported that *SGR1* mutants, like *nye1-1* in *Arabidopsis*, as well as loss-of-function mutants for some CCEs, such as HCAR, NYC1 and PPH, are nonfunctional type C stay-greens, i.e. they exhibit characteristics of normal senescence, but retain green color (Kusaba et al., 2007; Schelbert et al., 2009, 2013; Meguro et al., 2011). To examine whether *SGR2*-OX exhibits a functional or nonfunctional stay-green phenotype, we performed two types of experiments to examine senescence-related changes other than Chl breakdown. Using pulse amplitude modulated (PAM), at first we compared Minimum fluorescence ( $F_0$ ) and Maximum fluorescence ( $F_m$ ) of photosystem II (PSII), and maximum photochemical efficiency ( $F_v/F_m$ ) of PSII in dark-adapted leaves. During natural senescence (at 5 and 6 WAG),  $F_v/F_m$  ratios of *SGR2*-OX leaves were slightly lower than those of wild-type leaves (**Supplemental Figure 8A**). Although the  $F_m$  value of *SGR2*-OX was almost the similar as WT at every phase (3-6 week-old), the  $F_0$  value of *SGR2*-OX during senescence was significantly higher than that of WT (**Supplemental Figure 8B and 8C**), and it led to the slight decrease of  $F_v/F_m$  ratio of *SGR2*-OX. Second, leaf ion leakage was measured during dark-induced

senescence. Ion leakage was higher in *SGR2*-OX than in wild type, but similar to *SGR1*-OX (**Figure 2E**). These results indicate that *SGR2*-OX is a nonfunctional type C stay-green line that shows typical senescence changes, but retains Chl.

### **Mutations in the Two *SGR* Genes Cause Different Phenotypes under Dark-Induced Senescence Conditions**

To analyze the effect of mutations in the two *SGR* genes on Chl breakdown, we compared the rates of leaf yellowing in *nye1-1* and *sgr2-1* of *Arabidopsis* under dark-induced senescence conditions. A stay-green phenotype has been reported previously for *nye1-1*, which has a nonsense mutation in *SGR1* (Ren et al., 2007). Absence of *SGR2* transcripts was confirmed in the T-DNA insertion line *sgr2-1* (SALK\_003830C; Aubry et al., 2008), indicating it to represent a true knockout line (**Supplemental Figure 9**). Like the two *SGR*-OX plants described above, the two *sgr* mutants grew normally during vegetative stages without any obvious visible phenotype (**Figure 3A**, upper panel). After 6 DDI, however, *sgr2-1* exhibited early leaf yellowing during dark-induced senescence (**Figure 3A** and **3B**, lower panel), which is opposite to the phenotype of *SGR2*-OX (**Figure 2A**). For more reliability, we grew OX plants and mutants of two *SGRs* in the same tray and check the phenotype during DIS. At 6 DDI, *SGR1*-OX and *sgr2-1* similarly showed early leaf yellowing phenotype, while *SGR2*-OX and *nye1-1* showed stay-green phenotype (**Supplemental Figure 10**). These results indicate that the respective abundance of *SGR1* and *SGR2* directly affects the rate of Chl degradation during leaf senescence. We subsequently generated an *nye1-1 sgr2-1* double mutant. Leaf stay-greenness in *nye1-1 sgr2-1* was comparable to *nye1-1* leaves during dark-induced senescence (**Figure 3A** and **3B**), indicating that *SGR2* mainly functions to alleviate the *SGR1* activity in senescing *Arabidopsis* leaves.

### **Divergent Roles of *SGR2* in Abiotic Stress-Induced Chl Degradation**

Besides senescence, Chl degradation is also caused by several abiotic stress conditions (Lim et al., 2007). Although a relation of *SGR1* to disease-induced leaf chlorosis has been reported (Mur et al., 2010; Mecey et al., 2011), the roles of the two *SGRs* in abiotic stress-induced senescence remain undetermined.

Molecular mechanisms of salt-induced senescence have been widely studied in *Arabidopsis* using functional stay-green mutants that are deficient in NAC transcription factors (Balazadeh et al., 2010; Wu et al., 2012; Kim et al., 2013). Thus, we first examined leaf phenotypes of the two *SGR*-OX plants under salt stress conditions. After 6 d of salt treatment, *SGR1*-OX showed an accelerated leaf yellowing phenotype (**Figure 4A**). Consistent with the visible phenotype, total Chl levels dramatically decreased in *SGR1*-OX leaves (**Figure 4B**) accompanied by higher ion leakage rates (**Figure 4C**). On the other hand, *SGR2*-OX leaves retained greenness and higher Chl levels (**Figure 4A** and **4B**), but



showed no difference in ion leakage (**Figure 4C**). We also checked leaf phenotypes of the two *sgr* mutants under salt stress conditions. After 3 d of salt treatment, *sgr2-1* showed early leaf yellowing, while *nye1-1* leaves stayed green with highly retained Chl (**Supplemental Figure 11**), indicating that, besides dark-induced Chl degradation, SGR2 also interferes with salt-induced Chl degradation.

We further analyzed leaf phenotypes of the two *SGR*-OX plants under other abiotic stress conditions, such as drought, heat and high light. Under these stresses, *SGR1*-OX plants exhibited severe leaf yellowing (for drought stress, **Supplemental Figure 12**; for heat stress, **Supplemental Figure 13**; for high light stress, **Supplemental Figure 14**). On the other hand, we found that *SGR2*-OX plants consistently exhibited a stay-green phenotype under these stress conditions (**Figure 3A**; **Supplemental Figures 12-14**), indicating that SGR2 is negatively involved in the regulation of both senescence- and stress-induced Chl breakdown.

### **Altered Expression of CCE Genes by Overexpression or Mutations in *SGR1* and *SGR2***

To analyze whether, or to what extent modulation of gene expression of *SGR1* and *SGR2* may affect the expression of *NYC1* and *PPH* whose mutants display a stay-green phenotype (Horie et al. 2009; Schelbert et al. 2009), their transcript abundance was analyzed in the overexpressing or knockout mutant lines during dark-induced senescence. Expression levels of *NYC1* and *PPH* were significantly down-regulated in the *SGR2*-OX and *nye1-1* stay-green lines, and up-regulated in the early yellowing lines *SGR1*-OX and *sgr2-1* (**Figure 5**), indicating that SGR1 positively and SGR2 negatively influence the expression of the senescence-induced CCE genes, *NYC1* and *PPH*, consistent with the dark-induced senescence phenotypes of the corresponding overexpression and mutant lines. However, the mechanism of this regulation remains elusive.

### **SGR2 Interacts with LHCII at the Thylakoid Membrane**

We previously showed that *Arabidopsis* SGR1 localizes to the thylakoid membrane of chloroplasts and interacts with LHCII (Sakuraba et al., 2012b). To confirm chloroplast localization of SGR2, as predicted by ChloroP 1.1 (<http://www.cbs.dtu.dk/services/ChloroP/>), we produced *Arabidopsis* transgenic plants that carried a *P35S:SGR2-GFP* construct (**Supplemental Table 1**). In the cotyledon chloroplasts of transgenic plants, GFP fluorescence overlapped with red Chl autofluorescence as well as chloroplast targeted GFP protein (**Figure 6A**), and SGR2-GFP was mostly detected in membrane-enriched fractions of protein extracts from mature leaves (**Figure 6B**), indicating that like SGR1, SGR2 also localizes at the thylakoid membrane.

To examine whether SGR2 interacts with LHCII, we performed *in vivo* pull-down assays using SGR2-GFP transgenic plants. Our analysis revealed that both SGR1 and SGR2 co-immunoprecipitated LHCII subunits (Lhcb1, Lhcb2 and Lhcb4), but not CP43 or Lhca1 (**Figure 6C**).

We also analyzed the pulled-down lysate by silver staining of SDS-PAGE gel. We detected two strong bands (**Supplemental Figure 15A**). One is corresponding to SGR1-GFP or SGR2-GFP (**Supplemental Figure 15B**), and the other one is corresponding to the Major LHCII (**Supplemental Figure 15C**). These results indicate that like SGR1, SGR2 also strongly binds to LHCII at the thylakoid membrane.

### **SGR1 and SGR2 Have Different Capacities for Interaction with CCEs**

Previously, we demonstrated by yeast two-hybrid and bimolecular fluorescence complementation assays that SGR1 physically interacts with the six known CCEs (NOL, NYC1, HCAR, PPH, PAO and RCCR) directly or indirectly at LHCII (Sakuraba et al., 2012b; 2013). Because the phenotypes of *SGR2-OX* and mutant lines were opposite to those of *SGR1*-modulated plants under various senescence-inducing conditions, we considered the possibility that the interaction capacity of SGR2 with CCEs could be different from SGR1.

At first, we examined the pairwise interaction of the two SGRs with CCEs using yeast two-hybrid assays. This analysis revealed that the CCE interaction capacity of SGR2 was considerably limited compared to SGR1, except for its interaction with RCCR (**Figure 7A**). We further examined these pairwise interactions by *in vivo* pull-down assays using CCE antibodies (**Figure 7B**) or *in vitro* pull-down assays using GFP- or FLAG-tagged transgenic lines (**Figure 7C**). As reported previously (Sakuraba et al. 2012b), leaf samples used for these series of pull-down assays were senescence-induced by 3 DDI, and membrane-enriched fractions were treated with  $\alpha$ -GFP conjugated beads. Results of these pull-down assays were consistent with the yeast two-hybrid results (**Figure 7A**). Based on these results, we concluded that the distinct senescence phenotypes of the two *SGR-OX* lines and two *sgr* mutants are related to the difference in the interaction capacity of each SGR with CCEs.

### **The Two SGR Proteins Form Homo- or Heterodimers**

The two SGR proteins are considerably similar to each other (**Supplemental Figure 3**). Because several pairs of two similar proteins have been shown to form heterodimers for controlling their physiological functions (Seo et al. 2011, 2012), we speculated that the two SGR proteins possibly interact with each other. To examine this possibility, we checked the pairwise interactions between the two SGR homologs by yeast two-hybrid assays. Each SGR had the capacity of forming heterodimers with the other SGR but also to homodimerize with itself (**Figure 8A**). The pairwise interactions were further confirmed by *in vitro* pull-down assays using the C-terminal GFP- or FLAG-tagged SGR transgenic lines. To avoid the possibility of indirect interaction between them via LHCII subunits, one-week-old etiolated seedlings were used for these experiments. Consistent with the yeast two-

hybrid results, we confirmed the physical interactions of SGR1-SGR1, SGR1-SGR2, and SGR2-SGR2 (**Figure 8B-D**). These results strongly suggest that the two SGR proteins can form either homo- or heterodimers.

## DISCUSSION

Most higher plants have two or three SGR homologs, belonging to two subfamilies, SGR and SGRL. The physiological function of orthologs of the senescence-induced *Arabidopsis* SGR1/NYE1 has been widely studied in different plant species (Ren et al., 2007; Park et al., 2007; Barry et al., 2008; Sato et al., 2007), and a possible function of SGRL in Chl breakdown during vegetative growth has also been reported in rice (Rong et al., 2013). The *Arabidopsis thaliana* genome harbors two *SGR* homologs, *SGR1* and *SGR2* (**Supplemental Figures 1 and 2**). Although the expression patterns of *Arabidopsis* *SGR1* and *SGR2* are considerably similar throughout development (Breeze et al., 2011; **Figure 1**), detailed functional studies on SGR2 were still limited, because the *sgr2-1* knockout mutant did not show a stay-green phenotype (Aubry et al., 2008) but slightly earlier leaf yellowing in dark-induced senescence (**Figure 3**). By contrast, *Arabidopsis nye1-1* single mutants largely prevent Chl catabolism and display a stay-green phenotype (Ren et al., 2007) despite an up-regulation of *SGR2* in senescing *nye1-1* leaves (data not shown) as wild type (**Figure 1**). This suggested that the role of SGR2 is distinct from SGR1 in senescing *Arabidopsis* leaves.

Here, we examined potential physiological and biochemical roles of *Arabidopsis* SGR2, and uncovered that its function in Chl metabolism is antagonistic to SGR1, i.e. SGR2 acts as a negative regulator of Chl catabolism during leaf senescence (**Figure 2A-C**). This was rather unexpected, because the amino acid sequences of SGR1 and SGR2 are highly similar (76% sequence similarity) (**Supplemental Figures 1 and 2A**); thus, it is likely that these two sequences diverged from a common ancestor during evolution. Our results uncovered a possible mechanism for the opposite functions of SGR1 and SGR2 in Chl metabolism. In yeast two-hybrid and *in vivo* or *in vitro* pull-down assays, SGR1 physically interacted with all CCEs, but the SGR2 interaction with CCEs was almost absent, except for RCCR (**Figure 7**). Considering that SGR2 can interact with LHCII subunits (**Figure 6C**), it can be speculated that SGR2 also locates close to CCEs at the thylakoid membrane, and probably interrupts or reduces the formation of SGR1-CCE-LHCII complexes (Sakuraba et al., 2012b). This may allow *Arabidopsis* plant to better coordinate Chl breakdown with other cellular processes of senescence. A similar case was reported for two *Arabidopsis* homologs, FLOWERING LOCUS T (FT) and TERMINAL FLOWER1 (TFL1), which share 59% protein sequence similarity but act as an inducer and repressor of flowering, respectively (Hanzawa et al., 2005). Strikingly, swapping a single amino acid residue was shown to be sufficient to functionally convert FT to TFL1

and *vice versa*. It was suggested that this key residue contributes to the induction of flowering by affecting the interaction of FT and TFL1 with common interacting partners, such as FLOWERING LOCUS D, a bZIP transcription factor (Hanzawa et al., 2005; Ahn et al., 2006). Thus, the identification of amino acid residues of SGR1 and SGR2 that are important for binding to both LHCI and CCEs may provide a molecular basis for the regulation of Chl degradation by SGRs.

We also revealed by yeast two-hybrid and *in vitro* pull-down assays that *Arabidopsis* SGR1 and SGR2 form homo- or heterodimers (**Figure 8**). Thus, it is highly possible that heterodimer formation alleviates the formation of SGR1-CCE complex. For example, the interaction of SGR1 with CCEs may become weak when heterodimerizing with SGR2 because of its limited interaction capacity with CCEs. Similar regulation mechanisms of protein activity have been reported previously. Splicing variant (*CCA1b*) of *Arabidopsis* CIRCADIAN CLOCK-ASSOCIATED 1 (*CCA1a*) inhibits the formation of CCA1a homodimers by forming CCA1a-CCA1b heterodimers (Seo et al., 2012). Because of this negative regulation by heterodimerization, *Arabidopsis* *CCA1b*-OX plants showed a distinct phenotype from *CCA1a*-OX plants. For example, *CCA1a*-OX showed tolerance to freezing stress, while *CCA1b*-OX became cold sensitive (Seo et al., 2012). The *Arabidopsis* INDETERMINATE DOMAIN 14 transcription factor has a similar self-regulatory mechanism by forming heterodimers with its splicing variant (Seo et al., 2011). Considering these previous reports, it is highly possible that SGR1 activity is negatively regulated by heterodimerization with SGR2 during leaf senescence and Chl degradation-inducing stress conditions; *SGR2*-OX plants may mainly form inactive SGR1-SGR2 heterodimers and SGR2-SGR2 homodimers, but barely active SGR1-SGR1 homodimers.

Interestingly, the contribution of SGR2 to embryo degreening seems to be different from Chl degradation during leaf senescence. Delmas et al. (2013) recently reported that levels of Chl retention are much higher in *sgr1-1 sgr2-2* seeds than in *sgr1-1* (an allele distinct to *nye1-1*) seeds, indicating that SGR2 is involved in embryo degreening. One possibility is that SGR1 and SGR2-dependent Chl degradation during embryo degreening is mechanistically different from that during leaf senescence, because expression levels of some CCE genes, such as *HCAR*, *NOL* and *RCCR*, are considerably low during seed ripening (data not shown), as confirmed in the *Arabidopsis* eFP browser (<http://bbc.botany.utoronto.ca/efp/cgi-bin/efpWeb.cgi>). Furthermore, we consistently observed that the mature embryos of *SGR2*-OX seeds are normally yellow as wild-type seeds (data not shown). The soybean genome also contains two *SGR* homologs and one *SGRL* gene (**Supplemental Figures 1 and 2**). In contrast to our data in *Arabidopsis*, the two soybean *SGR* homologs, *D1/SGR1* (*Glyma01g42390*) and *D2/SGR2* (*Glyma11g02980*), have a duplicate gene function to activate Chl degradation during leaf senescence, as confirmed by constitutive expression in *Arabidopsis* *nye1-1* plants (Fang et al., 2014). Moreover, the *d1d2* double mutant exhibits a functional type B stay-green phenotype, which is quite different from the nonfunctional type C phenotypes found in *sgr1* mutants of different plant species. It can be speculated that after duplication, the developmental, biochemical

and physiological functions of *SGR* genes in Chl metabolism have been diversified during different evolution processes of each plant species. In line with this is the proposed role of *Medicago truncatula* *SGR* in root nodule senescence (Zhou et al., 2011). Therefore, the precise functions of *SGR* homologs in each plant species need to be tested experimentally *in vivo* in order to elucidate whether they act synergistically, redundantly, or antagonistically in Chl breakdown and/or other physiological processes.

In this study, we found that expression of the senescence-induced CCE genes, *NYC1* and *PPH*, is significantly down-regulated in *SGR2*-OX, contributing to the stay-green phenotype of these lines, but these genes are up-regulated in *SGR1*-OX, a line with accelerated leaf yellowing (**Figure 5**). These results strongly suggest that altering *SGR* abundance or *SGR*-related changes in photosystem balance or its pigment (Chl and carotenoid) composition in chloroplasts may affect nuclear gene expression during leaf senescence. Changes in nuclear gene expression have previously been reported to occur in an *Arabidopsis* stay-green line termed BCG (Sakuraba et al., 2012a). In BCG plants, the balance of photosystem core and antenna is different from wild type due to Chl *b* over-accumulation caused by the overexpression of chlorophyllide *a* oxygenase (Sakuraba et al., 2010). Thus, changes in the homeostasis of photosystem components may be signaled to the nucleus and may alter the expression of senescence-related genes. Similarly, it is possible that altered interactions of *SGRs* with LHCII perturb photosystem complexes and induce retrograde signal(s) from the chloroplast to the nucleus. Considering the results of this study, antagonistic functions of *SGR2* and *SGR1* in *Arabidopsis* may have evolved for the necessity of tightly controlling Chl catabolism in accordance with the dismantling and remobilizing process of cellular components during leaf senescence, which is different from the redundant functions of D1/*SGR1* and D2/*SGR2* in soybean (Fang et al., 2014).

## METHODS

### Plant Materials

*Arabidopsis thaliana* ecotype Columbia-0 (Col-0) was used as wild type. Full-length cDNAs of *SGR1* and *SGR2* in *Arabidopsis* (without stop codon for the C-terminal epitope-tagging) were amplified by RT-PCR using total RNA. After insertion of the *SGR1* and *SGR2* cDNAs into the Gateway entry vector pCR8/GW/TOPO (Invitrogen), the inserts were recombined into the binary Gateway vectors pEarleyGate 103, 202 and 205 for introducing C-terminal GFP, FLAG and TAP tags, respectively (Earley et al., 2006). The primers used for cloning are listed in **Supplemental Table 2**. *Arabidopsis* transgenic plants were obtained by *Agrobacterium tumefaciens* (strain GV3101)-mediated

transformation by a floral dipping method (Zhang et al., 2006). Primary transformants were selected on agar plates containing appropriate antibiotics. Lines that showed high expression of transgene were selected, and their third generation was subjected for further analysis. As a negative control for *in vivo* pull-down assays, transgenic plants carrying *P35S::GFP* were used (Sakuraba et al., 2012b). The T-DNA insertion-derived *sgr2-1* mutant (SALK\_003830C; Aubry et al., 2008) was obtained from the Arabidopsis Biological Resource Center (ABRC, Ohio State University, USA) (**Supplemental Figure 9**). The absence of *SGR2* mRNA in each mutant was confirmed by RT-PCR, and *ACTIN2* (*ACT2*; At3g18780) was used as a loading control (**Supplemental Figure 9**). For an *SGR1* mutant, *nye1-1* was used (Ren et al., 2007).

### **Growth Conditions**

*Arabidopsis* wild-type and transgenic plants were grown on soil in a growth chamber at 20°C (minimum temperature during nighttime) to 24°C (maximum temperature during daytime) under cool-white fluorescent light (90-100  $\mu\text{mol m}^{-2} \text{s}^{-1}$ ) in long-day (LD; 16-h light/8-h dark) conditions. Green rosette leaves detached from 3- or 4-week-old plants were sampled for dark-induced senescence and abiotic stress treatments. Detached leaves were incubated in light or in darkness at 22°C on 3 mM MES (pH 5.8) buffer with supplements, as indicated in the Figures. For dark-induced senescence treatment of whole plants, 3-week-old plants were transferred to complete darkness. After dark incubation, rosette leaves were sampled under dim green light. 2nd or 3rd rosette leaves were used for all experiments, including, Chl quantification, Ion leakage rate and Fv/Fm measurements, immunoblot analysis, and qRT-PCR analysis.

### **Pigment Analysis**

Total Chl was extracted from rosette leaves (2nd or 3rd) using ice-cold acetone at 4°C. Supernatants were diluted with ice-cold water to a final acetone concentration of 80%. Chl was quantified spectrophotometrically as previously described (Lichtenthaler, 1987).

### **Laser Scanning Confocal Microscopy**

GFP fluorescence images were recorded with a laser scanning confocal microscope (LSM510, Zeiss). An argon laser (25 mW) was used for generating an excitation source at 488 nm. GFP and Chl fluorescence were recorded at 525 nm and 660 nm, respectively.

### **Fluorescence Measurement of Fv/Fm using Pulse Amplitude Modulation (PAM)**

Maximal photochemical efficiency of photosystem II (Fv/Fm) was measured using a PAM 2000 fluorometer (Heinz Walz, Germany). Plants were dark-adapted for 5 min and the Fv/Fm ratios of 2nd or 3rd rosette leaves were measured at 20°C.

#### **Measurement of Ion Leakage**

Ion leakage was measured as described previously (Fan et al., 1997) with minor modifications. Membrane leakage was determined by measurement of electrolytes (or ions) leaking from 2nd or 3rd detached leaves. Ten leaves from each treatment were immersed in 6 mL of 0.4 M mannitol at room temperature with gentle shaking for 3 h, and conductivity of the solution measured with a conductivity meter (CON6 METER, LaMOTTE Co., USA). Total conductivity was determined after sample incubation at 85°C for 20 min. The ion leakage is expressed as the percentage of initial conductivity divided by total conductivity.

#### **Gene Expression Analysis**

Gene expression levels were measured by reverse transcription and quantitative real-time PCR (RT-qPCR) analysis. Total RNA was extracted from leaves using the Total RNA Extraction Kit including RNase-free DNase (iNtRON Biotechnology, Korea). For RT reactions, first-strand cDNA was synthesized from 5 µg of total RNA using M-MLV reverse transcriptase and an oligo(dT)<sub>15</sub> primer (Promega) in a 20 µL mixture. Then, the reaction was diluted to 100 µL with water, and used as template for qPCR analysis. The qPCR mixture (20 µL) contained 2 µL of first-strand cDNA template, 10 µL of LightCycler 480 SYBR Green I Master (Roche), and 0.25 µM of forward and reverse primers for each gene. Primer sets used for qPCR are listed in **Supplemental Table 2**. qPCR was performed using the Light Cycler 2.0 (Roche Diagnostics). Relative expression levels of each gene were normalized to those of *GAPDH* (glyceraldehyde phosphate dehydrogenase; At1g16300).

#### ***In vitro* and *In Vivo* Pull-Down Assays**

For the interaction of SGR homologs with CCEs or photosystem proteins, total leaf proteins were extracted from 3-week-old plants (3 DDI) and membrane-enriched fractions were purified using the Native Membrane Protein Extraction Kit (Calbiochem). To examine the interactions between SGR1 and SGR2, total proteins were extracted from 1-week-old etiolated seedlings using the Native Membrane Protein Extraction Kit (Calbiochem). Then, each extract was adjusted by Chl concentration, and pulled down using α-GFP-conjugated agarose beads (MBL, Japan) as described previously (Sakuraba et al., 2012b). The agarose beads were washed at least three times with washing

buffer (50 mM Tris-HCl [pH 7.2], 200 mM NaCl, 0.1% Nonidet P-40, 2 mM EDTA, and 10% glycerol). Washed beads were boiled with 20  $\mu$ L of sample buffer for 5 min and subjected to SDS-PAGE and immunoblot analysis.

### **SDS-PAGE, Silver staining, and Immunoblot Analysis**

Protein extracts or fractions of co-immunoprecipitation experiments were suspended with sample buffer (50 mM Tris-HCl [pH 6.8], 2 mM EDTA, 10% glycerol, 2% SDS, and 6% 2-mercaptoethanol), and denatured at 75°C for 3 min, and subjected to SDS-PAGE. The resolved proteins were electroblotted onto Immobilon-P transfer membranes (Millipore). For visualization of protein bands, gels or membranes were stained with Coomassie Brilliant Blue (Sigma-Aldrich). For visualization of co-immunoprecipitated samples, SilverQuest™ Silver Staining Kit (Invitrogen) were used according to the protocol. Antibodies against GFP (Abcam), FLAG (Cell Signaling, USA), NOL and NYC1 (Sato et al., 2009), RCCR (Pružinská et al., 2007), PAO and photosystem proteins (Lhcb1, Lhcb2, Lhcb4, Lhcb5, CytF, CP43 and D1) (Agrisera, Sweden) were used for protein detection. Peroxidase activity of secondary antibodies was visualized using the WEST SAVE chemiluminescence detection kit (AbFRONTIER, Korea).

### **Yeast Two-Hybrid Assays**

The full-length cDNA of *SGR2* in the entry vector pCR8/GW/TOPO was inserted into the destination vector pDEST32 as bait (Invitrogen). Bait (pDEST32) and prey (pDEST22) vectors of *SGR1* and *CCEs* have previously been prepared (Sakuraba et al., 2012b; Sakuraba et al., 2013). The yeast strain MaV203 was used for co-transformation of bait and prey clones, and  $\beta$ -galactosidase activity was measured by a liquid assay using chlorophenol red- $\beta$ -D-galactoside (CPRG; Roche Applied Science) according to the Yeast Protocol Handbook (Clontech).

### **Abiotic Stress Treatments**

Analysis of salt stress was performed as previously described with minor modifications (Wu et al., 2012). For analysis of salt stress-induced Chl degradation, 2nd or 3rd detached rosette leaves from 3-week-old plants were floated on 3 mM MES (pH 5.8) buffer containing 150 mM NaCl with the adaxial side-up, or 3-week-old plants grown on soil were supplied with 200 mM NaCl solution, and incubated for 3 d (detached leaves) or 6 d (whole plants) under continuous light conditions (CL; 22°C, 90-100  $\mu$ mol m<sup>-2</sup> s<sup>-1</sup>). For analysis of heat stress-induced Chl degradation, 3-week-old plants floating on 3 mM MES (pH 5.8) buffer containing 2 g/L Murashige and Skoog medium (Sigma-Adrich) were incubated for 4 h at 45°C and then transferred to 22°C for 72 h under long day (LD; 16-h light/8-h dark)



conditions. For analysis of drought stress-induced Chl degradation, 3 week-old plants were incubated in petri dishes without buffer at 23°C for 12 h, and then re-hydrated with water for 24 h under CL conditions.

**Accession Numbers** Sequence data from this article can be found in the Arabidopsis Genome Initiative (AGI) or GenBank/EMBL data libraries under the following accession numbers: *SGR1/NYE1* (At4g22920), *SGR2* (At4g11910), *NYC1* (At4g13250), *NOL* (At5g04900), *HCAR* (At1g04620), *PPH* (At5g13800), *PAO* (At3g44880), *RCCR* (At4g37000), *GAPDH* (At1g16300), and *ACT2* (At3g18780).

## SUPPLEMENTARY DATA

Supplementary Data are available at *Molecular Plant Online*.

## FUNDING

This work was supported by a grant (No. PJ009018) from the Next-Generation BioGreen 21 Program, Rural Development Administration, Korea (to N.-C.P) and a grant (No. 31003A\_132603) from the Swiss National Science Foundation (to S.H.).

## ACKNOWLEDGMENTS

We are most grateful to Dr. Ayumi Tanaka for providing antibodies against NOL and NYC1, and Dr. Benke Kuai for donating *nye1-1* seeds.

## Figure Legends

**Figure 1.** Expression Profiles of Three *Arabidopsis* SGR Homologs during Development or Under Dark-Induced Senescence Conditions.

Expression of *SGR1* (**A, D**), *SGR2* (**B, E**) and *SGRL* (**C, F**) was examined in 2nd and 3rd rosette leaves of wild-type (Col-0) plants during development (**A-C**) or in 2nd or 3rd detached rosette leaves from 3-week-old wild-type (Col-0) plants during dark-induced senescence (**D-F**). Plants were grown on soil at 22°C under long-day (16-h cool-white fluorescent light [90-100  $\mu\text{mol m}^{-2} \text{s}^{-1}$ ]/8-h dark) conditions. The relative expression levels of *SGR* genes were determined by RT-qPCR analysis and normalized to transcript levels of *GAPDH* (glyceraldehyde phosphate dehydrogenase; At1g16300). Mean and SD values were obtained from more than three biological replicates. These experiments were repeated at least twice with similar results. DDI, days of dark incubation.

**Figure 2.** Phenotypic Characterization of the Two *SGR*-OX Plants.

**(A)** Phenotypes of 3-week-old wild-type (WT) and the two *SGR*-OX plants before dark incubation (0 DDI) and after 8 DDI. Plants were grown on soil at 22°C in long-day conditions.

**(B)** Changes in total Chl levels in attached leaves (2nd or 3rd) of the plants in (A) before dark incubation (black), and after 4 DDI (gray) and 6 DDI (white). Means and SDs were obtained from three samples.

**(C)** Changes in photosynthetic protein levels in the leaves of plants like those shown in (A) before (0 DDI), and after 5 DDI and 8 DDI. Antibodies against photosystem II core (CP43 and D1), photosystem II antenna (Lhcb1, Lhcb2, Lhcb4 and Lhcb5), Lhca1, CytF and PAO were used. RbcL (Rubisco large subunit) was visualized by Coomassie Brilliant Blue staining after immunoblot analysis.

**(D)** Membrane ion leakage (as percentage of total ions) of detached leaves from WT and the two *SGR*-OX lines before dark treatment (0 DDI; black), and after 5 (gray) or 8 (white) DDI. Green rosette leaves of 4-week-old plants were used.

**(B, D)** A Student's *t*-test was used to calculate pairwise statistical significance (\**P*<0.05, \*\**P*<0.01). Means and SDs were obtained from more than seven leaf samples. All of these experiments were repeated more than twice with similar results. DDI, days of dark incubation; *S1*-OX, *SGR1*-OX; *S2*-OX, *SGR2*-OX.

**Figure 3.** Phenotypic Characterization of Single and Double Mutants in *SGR1* and *SGR2* during Dark-Induced Senescence.

Phenotypes (A) and total Chl levels (B) of 3-week-old *nye1-1*, *sgr2-1*, *nye1-1 sgr2-1* mutants before (0 DDI; upper panel) and after 6 d of dark incubation (6 DDI; lower panel). Means and SDs were obtained from more than seven samples. A Student's *t*-test was used to calculate pairwise statistical significance (\**P*<0.05, \*\**P*<0.01). These experiments were repeated more than twice with similar results.

**Figure 4.** Color Changes in Attached Leaves of the two *SGR*-OX Plants under Salt Stress.

**(A)** Visible phenotypes of wild-type (WT) and two *SGR*-OX plants after 6 d of salt treatment (200 mM NaCl). Three-week-old plants grown on soil under LD conditions were used. **(B, C)** Changes of total Chl levels (B) and ion leakage rates (C) in 6th rosette leaves of plants as shown in (A). Means and SDs were obtained from more than ten samples. A Student's *t*-test was used to calculate pairwise statistical significance (\**P*<0.05). These experiments were repeated more than twice with similar results. *S1*-OX, *SGR1*-OX; *S2*-OX, *SGR2*-OX.

**Figure 5.** Altered Expression of the Two CCE Genes *NYC1* and *PPH* in *SGR*-OX Plants and *sgr* Mutants during Dark-Induced Senescence.

Total RNA was extracted from the rosette leaves of 3-week-old plants before and after dark incubation (black, 0 DDI; gray, 3 DDI; white, 5 DDI). Relative expression levels of *NYC1* (A) and *PPH* (B) were determined by RT-qPCR and normalized to the transcript levels of *GAPDH*. Means and SDs were obtained from more than six samples. A Student's *t*-test was used to calculate pairwise statistical significance (\**P*<0.05, \*\**P*<0.01). These experiments were repeated twice with similar results. *S1-OX*, *SGR1-OX*; *S2-OX*, *SGR2-OX*.

**Figure 6.** SGR2 Interacts with LHCII at Thylakoid Membranes *In Vivo*.

(A) Chloroplast localization of SGR1-GFP (S1-GFP), and SGR2-GFP (S2-GFP). Cotyledons of 1-week-old WT (Negative control), transgenic plants expressing SGR-GFP fusions (SGR1-GFP and SGR2-GFP), and chloroplast targeted GFP (Positive control), were observed by laser scanning confocal microscopy. Red Chl autofluorescence (left), green GFP fluorescence (middle), and merged images (right) are shown. Bar = 50  $\mu$ m.

(B) SGR-GFP fusion proteins are more abundant in membrane-enriched protein fractions compared to soluble fractions. Total protein extracts were obtained from the rosette leaves of 3-week-old plants. GFP fusion proteins were detected by immunoblotting with an  $\alpha$ -GFP antibody (upper panel). After immunoblot analysis, membranes were stained with Coomassie Brilliant Blue (CBB) as loading control (lower panel).

(C) SGR2 interacts with LHCII subunits *in vivo*. Three-week-old plants expressing SGR-GFP fusions, i.e. SGR1-GFP (S1-GFP; positive control), SGR2-GFP (S2-GFP), and negative control (GFP) plants were incubated in darkness for 2 d. Membrane-enriched fractions were used for pull-down experiments using  $\alpha$ -GFP antibody-conjugated agarose beads (GFP-IP). Co-precipitated proteins were detected by immunoblotting using respective antibodies. Input, immunoblot analysis of the fractions used for GFP-IP. These experiments were repeated more than twice with similar results.

**Figure 7.** Physical Interactions of SGR1 and SGR2 with CCEs.

(A) Pairwise interactions of SGR1 and SGR2 with 6 CCEs in yeast two-hybrid assays. Relative  $\beta$ -galactosidase ( $\beta$ -Gal) activity was determined in liquid assays using chlorophenol red- $\beta$ -D-galactosidase (CPRG) as substrate. Empty prey plasmids (-) were used as negative controls. Mean and SD values were obtained from five independent colonies.

(B) Co-immunoprecipitation of CCEs (RCCR, NOL, NYC1, and PAO) and SGRs in senescing chloroplasts. SGR1-GFP (S1-GFP), SGR2-GFP (S2-GFP), and GFP (negative control) transgenic plants grown for 3 weeks under LD conditions were transferred to darkness and sampled at 3 DDI. Membrane-enriched fractions were used for *in vivo* pull-down assays. GFP was immunoprecipitated (GFP-IP) with  $\alpha$ -GFP-conjugated beads. RCCR, NOL, NYC1, and PAO in the input samples (left panel) and the pulled fractions (right panel) were detected using respective antibodies.

(C) Interactions between SGRs and PPH or HCAR by *in vitro* pull-down assays. Equal fresh weight of rosette leaves of 3-week-old transgenic *Arabidopsis* plants expressing FLAG-tagged SGRs and GFP-tagged HCAR or PPH (3 DDI) were co-homogenized. Membrane-enriched fractions were used for pull-down assays with  $\alpha$ -GFP-conjugated beads (GFP-IP), followed by immunoblot analysis using  $\alpha$ -FLAG. GFP transgenic plants were used as a negative control. These experiments were repeated more than twice with similar results.

**Figure 8. SGR1 and SGR2 Form Homo- or Heterodimers.**

(A) Pairwise interactions between SGR1 and SGR2. Relative  $\beta$ -galactosidase ( $\beta$ -Gal) activity was determined in liquid assays using chlorophenol red- $\beta$ -D-galactosidase (CPRG) as substrate. Empty bait plasmids (-) were used as negative controls. Means and SDs were obtained from five independent colonies.

(B-D) Interaction of SGR1 and SGR2 by *in vitro* pull-down assays. Equal fresh weight of 1-week-old etiolated seedlings of transgenic *Arabidopsis* lines expressing GFP-tagged SGR1 (S1-GFP) or SGR2 (S2-GFP) were co-homogenized with FLAG-tagged SGR1 (S1-FLAG) or SGR2 (S2-FLAG). Each homogenate was used for pull-down assays with  $\alpha$ -GFP-conjugated beads (GFP-IP), followed by immunoblot analysis using  $\alpha$ -FLAG. GFP transgenic plants were used as a negative control. The series of experiments was performed more than twice with similar results.

## REFERENCES

- Ahn, J.H., Miller, D., Winter, V.J., Banfield, M.J., Lee, J.H., Yoo, S.Y., Henz, S.R., Brady, R.L., and Weigel, D. (2006). A divergent external loop confers antagonistic activity on floral regulators *FT* and *TFL1*. *EMBO J.* **25**, 605-614.
- Aubry, S., Mani, J., and Hortensteiner, S. (2008). Stay-green protein, defective in Mendel's green cotyledon mutant, acts independent and upstream of pheophorbide a oxygenase in the chlorophyll catabolic pathway. *Plant Mol. Biol.* **67**, 243-256.
- Balazadeh, S., Siddiqui, H., Allu, A.D., Matallana-Ramirez, L.P., Caldana, C., Mehrnia, M., Zanol, M.I., Köhler, B., and Mueller-Roeber, B. (2010). A gene regulatory network controlled by the NAC transcription factor ANAC092/AtNAC2/ORE1 during salt-promoted senescence. *Plant J.* **62**, 250-264.
- Barry, C.S., McQuinn, R.P., Chung, M.Y., Besuden, A., and Giovannoni, J.J. (2008). Amino acid substitutions in homologs of the STAY-GREEN protein are responsible for the green-flesh and chlorophyll retainer mutations of tomato and pepper. *Plant Physiol.* **147**, 179-187.
- Breeze, E., Harrison, E., McHattie, S., Hughes, L., Hickman, R., Hill, C., Kiddle, S., Kim, Y., Penfold, C.A., and Jenkins, D. (2011). High-resolution temporal profiling of transcripts during Arabidopsis leaf senescence reveals a distinct chronology of processes and regulation. *Plant Cell.* **23**, 873-894.
- Curtis, M.D., and Grossniklaus, U. (2003). A gateway cloning vector set for high-throughput functional analysis of genes in planta. *Plant Physiol.* **133**, 462-469.
- Delmas, F., Sankaranarayanan, S., Deb, S., Widdup, E., Bournonville, C., Bollier, N., Northey, J.G., McCourt, P., and Samuel, M.A. (2013). ABI3 controls embryo degreening through Mendel's I locus. *Proc. Natl. Acad. Sci. USA.* **110**, E3888-E3894.
- Earley, K.W., Haag, J.R., Pontes, O., Opper, K., Juehne, T., Song, K., and Pikaard, C.S. (2006). Gateway-compatible vectors for plant functional genomics and proteomics. *Plant J.* **45**, 616-629.
- Fan, L., Zheng, S., and Wang, X. (1997). Antisense suppression of phospholipase D alpha retards abscisic acid-and ethylene-promoted senescence of postharvest Arabidopsis leaves. *Plant Cell.* **9**, 2183-2196.
- Fang, C., Li, C., Li, W., Wang, Z., Zhou, Z., Shen, Y., Wu, M., Wu, Y., Li, G., Kong, L.A., Liu, C., Jackson, S.A., and Tian, Z. (2014). Concerted evolution of D1 and D2 to regulate chlorophyll degradation in soybean. *Plant J.* doi: 10.1111/tpj.12419.
- Greenberg, J.T., and Ausubel, F.M. (2002). Arabidopsis mutants compromised for the control of cellular damage during pathogenesis and aging. *Plant J.* **4**, 327-341.

- Greenberg, J.T., Guo, A., Klessig, D.F., and Ausubel, F.M.** (1994). Programmed cell death in plants: a pathogen-triggered response activated coordinately with multiple defense functions. *Cell*. **77**, 551-563.
- Hörtensteiner, S.** (2009). Stay-green regulates chlorophyll and chlorophyll-binding protein degradation during senescence. *Trends Plant Sci.* **14**, 155-162.
- Hörtensteiner, S., and Feller, U.** (2002). Nitrogen metabolism and remobilization during senescence. *J. Exp. Bot.* **53**, 927-937.
- Hörtensteiner, S., and Kräutler, B.** (2011). Chlorophyll breakdown in higher plants. *Biochim. Biophys. Acta.* **1807**, 977-988.
- Hanzawa, Y., Money, T., and Bradley, D.** (2005). A single amino acid converts a repressor to an activator of flowering. *Proc. Natl. Acad. Sci. USA.* **102**, 7748-7753.
- Hirashima, M., Tanaka, R., and Tanaka, A.** (2009). Light-independent cell death induced by accumulation of pheophorbide a in *Arabidopsis thaliana*. *Plant Cell Physiol.* **50**, 719-729.
- Horie, Y., Ito, H., Kusaba, M., Tanaka, R., and Tanaka, A.** (2009). Participation of chlorophyll *b* reductase in the initial step of the degradation of light-harvesting chlorophyll *a/b*-protein complexes in *Arabidopsis*. *J. Biol. Chem.* **284**, 17449-17456.
- Jiang, H., Li, M., Liang, N., Yan, H., Wei, Y., Xu, X., Liu, J., Xu, Z., Chen, F., and Wu, G.** (2007). Molecular cloning and function analysis of the stay green gene in rice. *Plant J.* **52**, 197-209.
- Kim, Y.S., Sakuraba, Y., Han, S.H., Yoo, S.C., and Paek, N.C.** (2013). Mutation of the *Arabidopsis* NAC016 transcription factor delays leaf senescence. *Plant Cell Physiol.* **54**, 1660-1672.
- Kusaba, M., Ito, H., Morita, R., Iida, S., Sato, Y., Fujimoto, M., Kawasaki, S., Tanaka, R., Hirochika, H., Nishimura, M., et al.** (2007). Rice NON-YELLOW COLORING1 is involved in light-harvesting complex II and grana degradation during leaf senescence. *Plant Cell.* **19**, 1362-1375.
- Lichtenthaler, H.K.** (1987). Chlorophylls and carotenoids: Pigments of photosynthetic biomembranes. *Methods Enzymol.* **148**, 350-382.
- Lim, P.O., Kim, H.J., and Gil Nam, H.** (2007). Leaf senescence. *Annu. Rev. Plant Biol.* **58**, 115-136.
- Mach, J.M., Castillo, A.R., Hoogstraten, R., and Greenberg, J.T.** (2001). The *Arabidopsis*-accelerated cell death gene *ACD2* encodes red chlorophyll catabolite reductase and suppresses the spread of disease symptoms. *Proc. Natl. Acad. Sci. USA* **98**, 771-776.
- Mecey, C., Hauck, P., Trapp, M., Pumplin, N., Plovanich, A., Yao, J., and He, S.Y.** (2011). A critical role of STAYGREEN/Mendel's I locus in controlling disease symptom development during *Pseudomonas syringae* pv tomato infection of *Arabidopsis*. *Plant Physiol.* **157**, 1965-1974.
- Meguro, M., Ito, H., Takabayashi, A., Tanaka, R., and Tanaka, A.** (2011). Identification of the 7-hydroxymethyl chlorophyll *a* reductase of the chlorophyll cycle in *Arabidopsis*. *Plant Cell.* **23**, 3442-3453.

- Morita, R., Sato, Y., Masuda, Y., Nishimura, M., and Kusaba, M.** (2009). Defect in non-yellow coloring 3, an  $\alpha/\beta$  hydrolase-fold family protein, causes a stay-green phenotype during leaf senescence in rice. *Plant J.* **59**, 940-952.
- Mur, L.A.J., Aubry, S., Mondhe, M., Kingston-Smith, A., Gallagher, J., Timms-Taravella, E., James, C., Papp, I., Hörtensteiner, S., and Thomas, H.** (2010). Accumulation of chlorophyll catabolites photosensitizes the hypersensitive response elicited by *Pseudomonas syringae* in *Arabidopsis*. *New Phytol.* **188**, 161-174.
- Park, S.Y., Yu, J.W., Park, J.S., Li, J., Yoo, S.C., Lee, N.Y., Lee, S.K., Jeong, S.W., Seo, H.S., Koh, H.J., et al.** (2007). The senescence-induced staygreen protein regulates chlorophyll degradation. *Plant Cell.* **19**, 1649-1664.
- Pružinská, A., Anders, I., Aubry, S., Schenk, N., Tapernoux-Luthi, E., Muller, T., Krautler, B., and Hortensteiner, S.** (2007). In vivo participation of red chlorophyll catabolite reductase in chlorophyll breakdown. *Plant Cell.* **19**, 369-387.
- Pružinská, A., Tanner, G., Anders, I., Roca, M., and Hortensteiner, S.** (2003). Chlorophyll breakdown: pheophorbide a oxygenase is a Rieske-type iron-sulfur protein, encoded by the accelerated cell death 1 gene. *Proc. Natl. Acad. Sci. USA.* **100**, 15259-15264.
- Ren, G., An, K., Liao, Y., Zhou, X., Cao, Y., Zhao, H., Ge, X., and Kuai, B.** (2007). Identification of a novel chloroplast protein AtNYE1 regulating chlorophyll degradation during leaf senescence in *Arabidopsis*. *Plant Physiol.* **144**, 1429-1441.
- Rong, H., Tang, Y., Zhang, H., Wu, P., Chen, Y., Li, M., Wu, G., and Jiang, H.** (2013). The Stay-Green Rice like (SGRL) gene regulates chlorophyll degradation in rice. *J. Plant Physiol.* **170**, 1367-1373.
- Sakuraba, Y., Balazadeh, S., Tanaka, R., Muller-Rober, B., and Tanaka, A.** (2012a). Overproduction of Chl *b* retards senescence through transcriptional reprogramming in *Arabidopsis*. *Plant Cell Physiol.* **53**, 505-517.
- Sakuraba, Y., Kim, Y.S., Yoo, S.C., Hortensteiner, S., and Paek, N.C.** (2013). 7-Hydroxymethyl chlorophyll *a* reductase functions in metabolic channeling of chlorophyll breakdown intermediates during leaf senescence. *Biochem. Biophys. Res. Commun.* **430**, 32-37.
- Sakuraba, Y., Schelbert, S., Park, S.Y., Han, S.H., Lee, B.D., Andrès, C.B., Kessler, F., Hörtensteiner, S., and Paek, N.C.** (2012b). STAY-GREEN and chlorophyll catabolic enzymes interact at light-harvesting complex II for chlorophyll detoxification during leaf senescence in *Arabidopsis*. *Plant Cell.* **24**, 507-518.
- Sakuraba, Y., Yokono, M., Akimoto, S., Tanaka, R., and Tanaka, A.** (2010). Deregulated chlorophyll *b* synthesis reduces the energy transfer rate between photosynthetic pigments and induces photodamage in *Arabidopsis thaliana*. *Plant Cell Physiol.* **51**, 1055-1065.
- Sato, Y., Morita, R., Katsuma, S., Nishimura, M., Tanaka, A., and Kusaba, M.** (2009). Two short-chain dehydrogenase/reductases, NON-YELLOW COLORING 1 and NYC1-LIKE, are required

- for chlorophyll b and light-harvesting complex II degradation during senescence in rice. *Plant J.* **57**, 120-131.
- Sato, Y., Morita, R., Nishimura, M., Yamaguchi, H., and Kusaba, M.** (2007). Mendel's green cotyledon gene encodes a positive regulator of the chlorophyll-degrading pathway. *Proc. Natl. Acad. Sci. USA.* **104**, 14169-14174.
- Schelbert, S., Aubry, S., Burla, B., Agne, B., Kessler, F., Krupinska, K., and Hörtensteiner, S.** (2009). Pheophytin pheophorbide hydrolase (pheophytinase) is involved in chlorophyll breakdown during leaf senescence in Arabidopsis. *Plant Cell.* **21**, 767-785.
- Scheumann, V., Schoch, S., and Rüdiger, W.** (1998). Chlorophyll a formation in the chlorophyll b reductase reaction requires reduced ferredoxin. *J. Biol. Chem.* **273**, 35102-35108.
- Seo, P.J., Kim, M.J., Ryu, J.Y., Jeong, E.Y., and Park, C.M.** (2011). Two splice variants of the IDD14 transcription factor competitively form nonfunctional heterodimers which may regulate starch metabolism. *Nat. Commun.* **2**, 303.
- Seo, P.J., Park, M.J., Lim, M.H., Kim, S.G., Lee, M., Baldwin, I.T., and Park, C.M.** (2012). A self-regulatory circuit of CIRCADIAN CLOCK-ASSOCIATED1 underlies the circadian clock regulation of temperature responses in Arabidopsis. *Plant Cell.* **24**, 2427-2442.
- Thomas, H., and Howarth, C.J.** (2000). Five ways to stay green. *J. Exp. Bot.* **51**, 329-337.
- Wei, Q., Guo, Y., and Kuai, B.** (2011). Isolation and characterization of a chlorophyll degradation regulatory gene from tall fescue. *Plant Cell Rep.* **30**, 1201-1207.
- Wu, A., Allu, A.D., Garapati, P., Siddiqui, H., Dortay, H., Zanol, M.I., Asensi-Fabado, M.A., Munné-Bosch, S., Antonio, C., Tohge, T., et al.** (2012). *JUNGBRUNNEN1*, a reactive oxygen species-responsive NAC transcription factor, regulates longevity in Arabidopsis. *Plant Cell.* **24**, 482-506.
- Zhang, X., Henriques, R., Lin, S.S., Niu, Q.W., and Chua, N.H.** (2006). Agrobacterium-mediated transformation of Arabidopsis thaliana using the floral dip method. *Nat. Protoc.* **1**, 641-646.
- Zhou, C., Han, L., Pislariu, C., Nakashima, J., Fu, C., Jiang, Q., Quan, L., Blancaflor, E.B., Tang, Y., and Bouton, J.H.** (2011). From model to crop: functional analysis of a STAY-GREEN gene in the model legume Medicago truncatula and effective use of the gene for alfalfa improvement. *Plant Physiol.* **157**, 1483-1496.



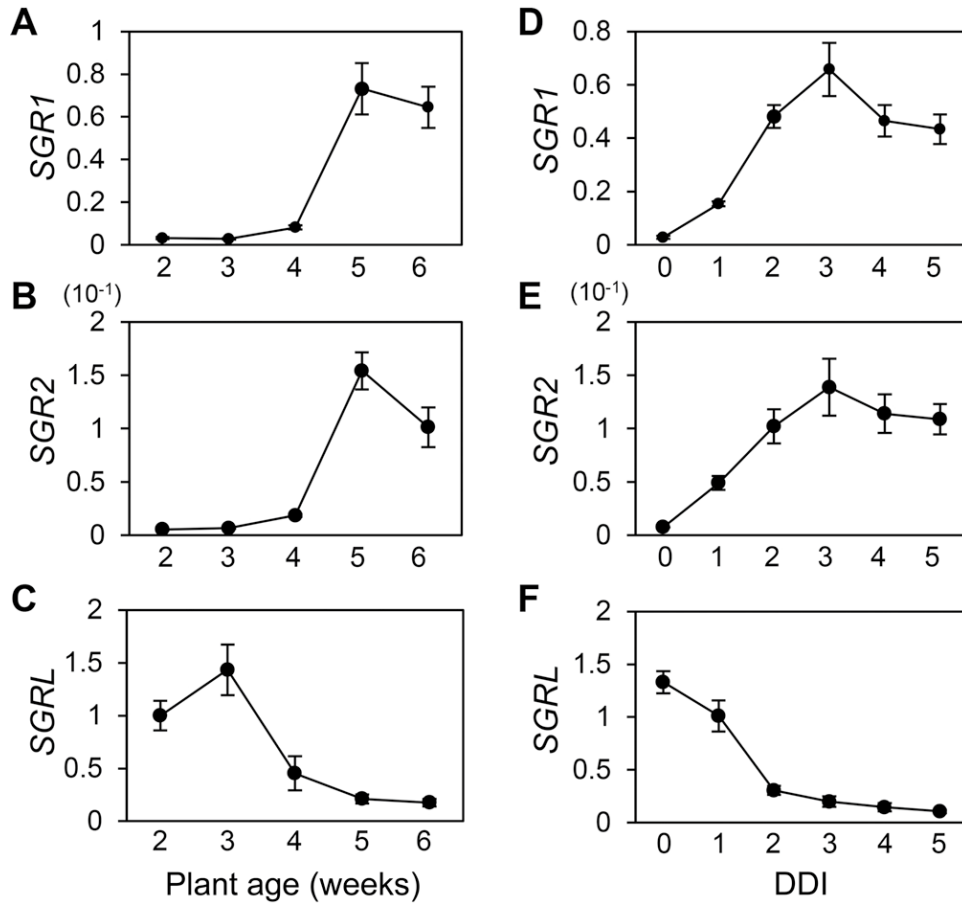


**Figure 1.** Expression Profiles of Three *Arabidopsis* *SGR* Homologs during Development or Under Dark-Induced Senescence Conditions.

Expression of *SGR1* (A, D), *SGR2* (B, E) and *SGRL* (C, F) was examined in 2nd and 3rd rosette leaves of wild-type (Col-0) plants during development (A-C) or in 2nd or 3rd detached rosette leaves from 3-week-old wild-type (Col-0) plants during dark-induced senescence (D-F). Plants were grown on soil at 22°C under long-day (16-h cool-white fluorescent light [90-100  $\mu\text{mol m}^{-2} \text{s}^{-1}$ ]/8-h dark) conditions. The relative expression levels of *SGR* genes were determined by RT-qPCR analysis and normalized to transcript levels of *GAPDH* (glyceraldehyde phosphate dehydrogenase; At1g16300). Mean and SD values were obtained from more than three biological replicates. These experiments were repeated at least twice with similar results. DDI, days of dark incubation.

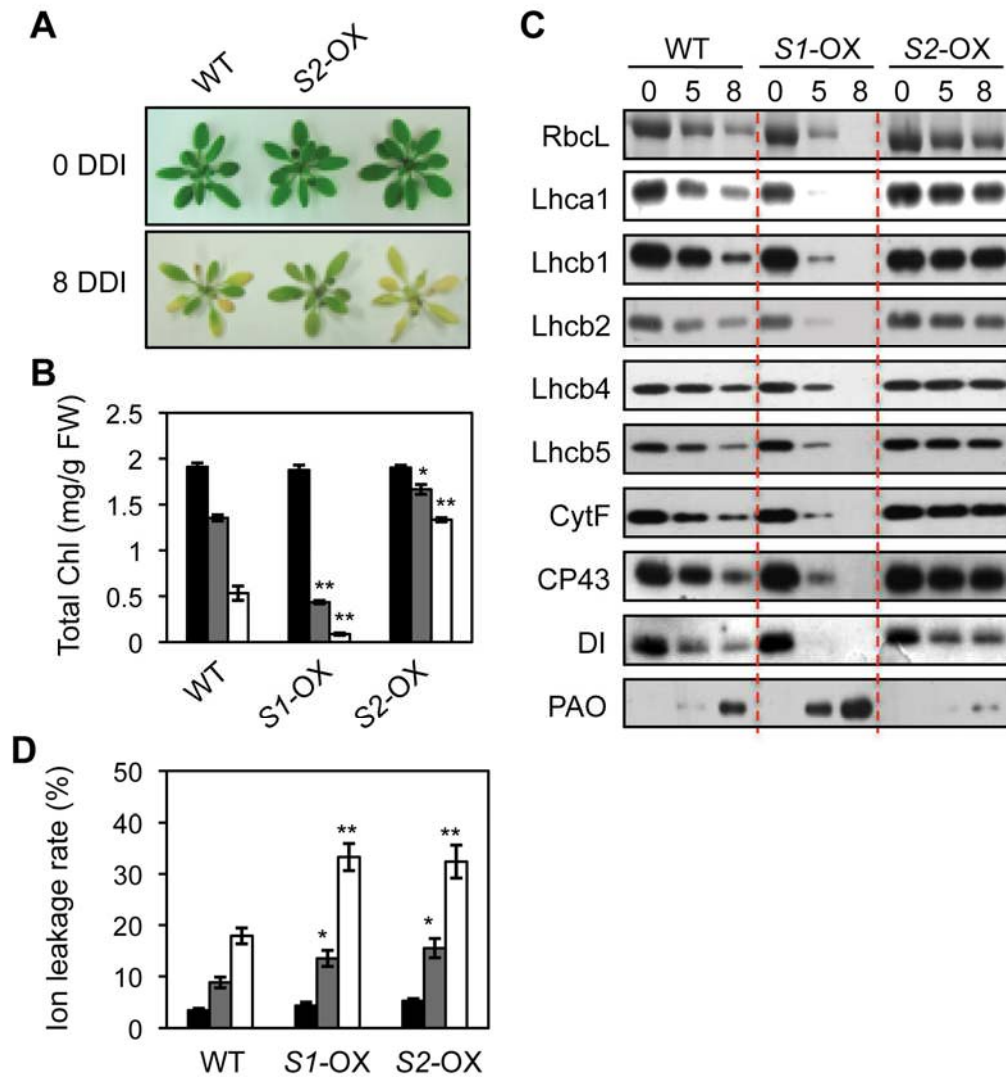


**Figure 2.** Phenotypic Characterization of the Two *SGR*-OX Plants.

**(A)** Phenotypes of 3-week-old wild-type (WT) and the two *SGR*-OX plants before dark incubation (0 DDI) and after 8 DDI. Plants were grown on soil at 22°C in long-day conditions.

**(B)** Changes in total Chl levels in attached leaves (2nd or 3rd) of the plants in (A) before dark incubation (black), and after 5 DDI (gray) and 8 DDI (white). Means and SDs were obtained from three samples.

**(C)** Changes in photosynthetic protein levels in the leaves of plants like those shown in (A) before (0 DDI), and after 5 DDI and 8 DDI. Antibodies against photosystem II core (CP43 and D1), photosystem II antenna (Lhcb1, Lhcb2, Lhcb4 and Lhcb5), Lhca1, CytF and PAO were used. RbcL (Rubisco large subunit) was visualized by Coomassie Brilliant Blue staining after immunoblot analysis.

**(D)** Membrane ion leakage (as percentage of total ions) of detached leaves from WT and the two *SGR*-OX lines before dark treatment (0 DDI; black), and after 5 (gray) or 8 (white) DDI. Green rosette leaves of 4-week-old plants were used.

**(B, D)** A Student's *t*-test was used to calculate pairwise statistical significance (\* $P < 0.05$ , \*\* $P < 0.01$ ). Means and SDs were obtained from more than seven leaf samples. All of these experiments were repeated more than twice with similar results. DDI, days of dark incubation; *S1*-OX, *SGR1*-OX; *S2*-OX, *SGR2*-OX.

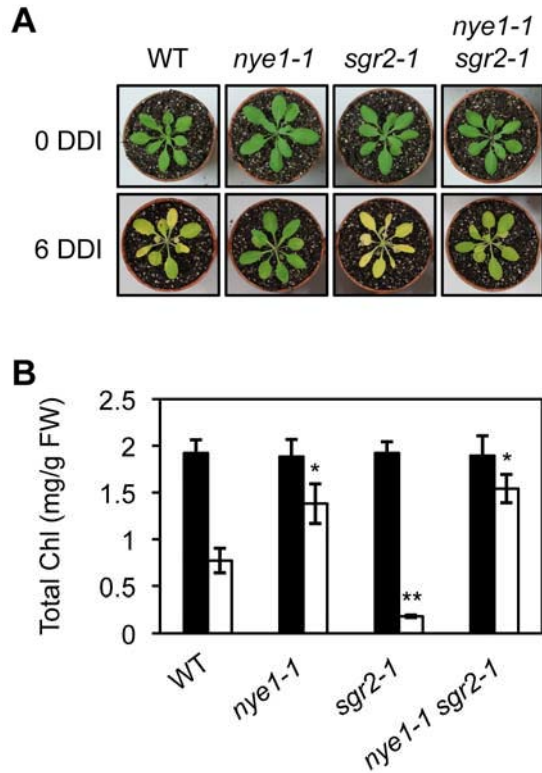


**Figure 3.** Phenotypic Characterization of Single and Double Mutants in *SGR1* and *SGR2* during Dark-Induced Senescence.

Phenotypes (A) and total Chl levels (B) of 3-week-old *nye1-1*, *sgr2-1*, *nye1-1 sgr2-1* mutants before (0 DDI; upper panel) and after 6 d of dark incubation (6 DDI; lower panel). Means and SDs were obtained from more than seven samples. A Student's *t*-test was used to calculate pairwise statistical significance (\* $P < 0.05$ , \*\* $P < 0.01$ ). These experiments were repeated more than twice with similar results.

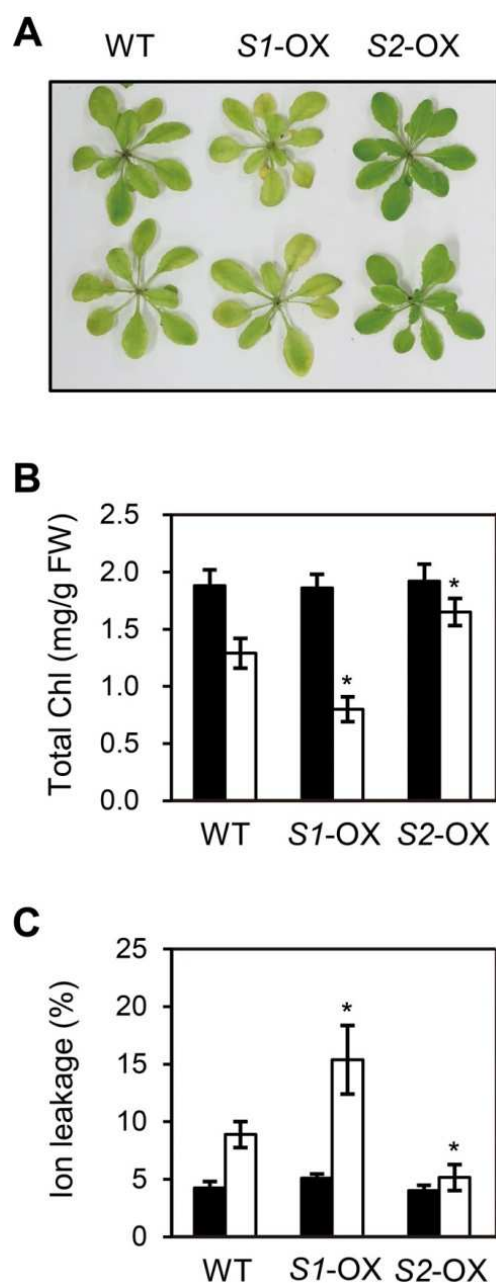


**Figure 4.** Color Changes in Attached Leaves of the two *SGR*-OX Plants under Salt Stress.

(A) Visible phenotypes of wild-type (WT) and two *SGR*-OX plants after 6 d of salt treatment (200 mM NaCl). Three-week-old plants grown on soil under LD conditions were used. (B, C) Changes of total Chl levels (B) and ion leakage rates (C) in 6th rosette leaves of plants as shown in (A). Means and SDs were obtained from more than ten samples. A Student's *t*-test was used to calculate pairwise statistical significance (\* $P < 0.05$ ). These experiments were repeated more than twice with similar results. *S1*-OX, *SGR1*-OX; *S2*-OX, *SGR2*-OX.

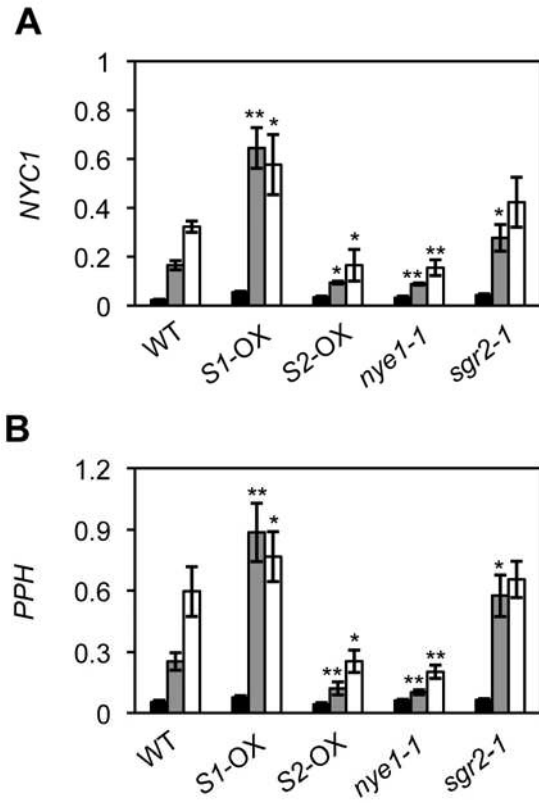


**Figure 5.** Altered Expression of the Two CCE Genes *NYC1* and *PPH* in *SGR*-OX Plants and *sgr* Mutants during Dark-Induced Senescence.

Total RNA was extracted from the rosette leaves of 3-week-old plants before and after dark incubation (black, 0 DDI; gray, 3 DDI; white, 5 DDI). Relative expression levels of *NYC1* (A) and *PPH* (B) were determined by RT-qPCR and normalized to the transcript levels of *GAPDH*. Means and SDs were obtained from more than six samples. A Student's *t*-test was used to calculate pairwise statistical significance (\* $P < 0.05$ , \*\* $P < 0.01$ ). These experiments were repeated twice with similar results. *S1*-OX, *SGR1*-OX; *S2*-OX, *SGR2*-OX.

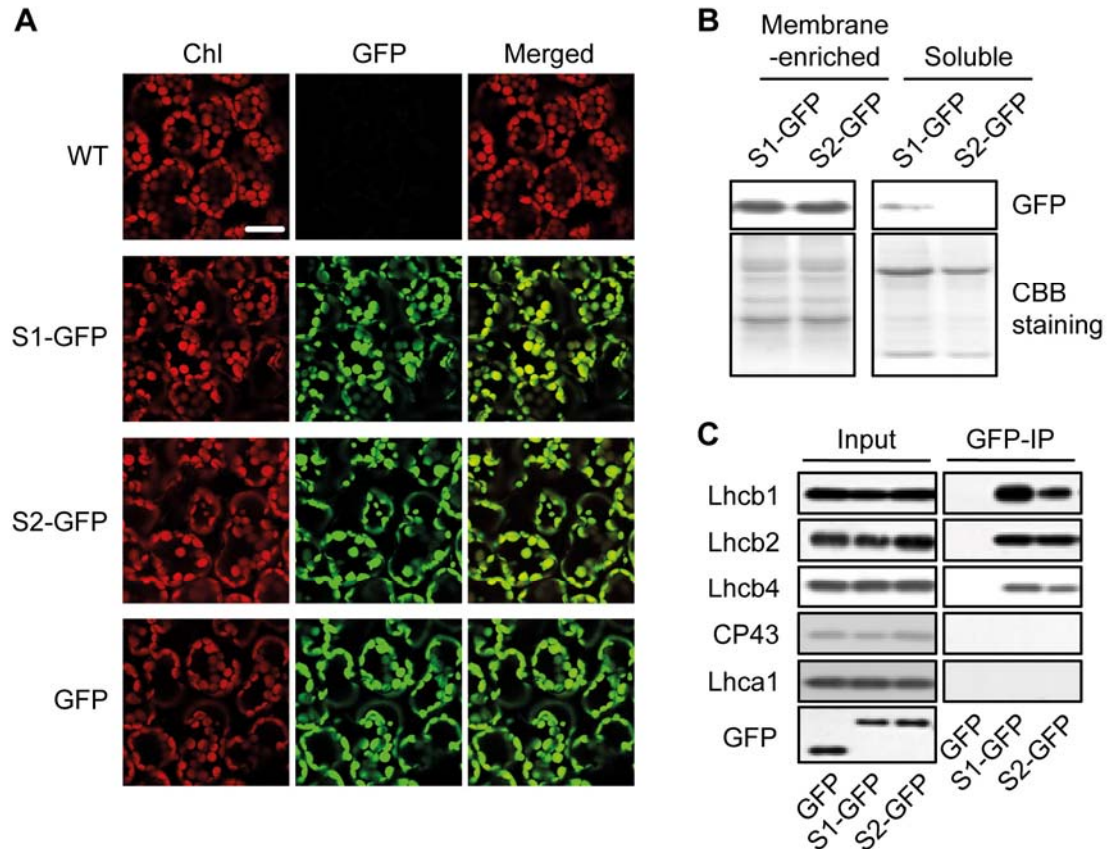


**Figure 6.** SGR2 Interacts with LHCII at Thylakoid Membranes *In Vivo*.

(A) Chloroplast localization of SGR1-GFP (S1-GFP), and SGR2-GFP (S2-GFP). Cotyledons of 1-week-old WT (Negative control), transgenic plants expressing SGR-GFP fusions (SGR1-GFP and SGR2-GFP), and chloroplast targeted GFP (Positive control), were observed by laser scanning confocal microscopy. Red Chl autofluorescence (left), green GFP fluorescence (middle), and merged images (right) are shown. Bar = 50  $\mu$ m.

(B) SGR-GFP fusion proteins are more abundant in membrane-enriched protein fractions compared to soluble fractions. Total protein extracts were obtained from the rosette leaves of 3-week-old plants. GFP fusion proteins were detected by immunoblotting with an  $\alpha$ -GFP antibody (upper panel). After immunoblot analysis, membranes were stained with Coomassie Brilliant Blue (CBB) as loading control (lower panel).

(C) SGR2 interacts with LHCII subunits *in vivo*. Three-week-old plants expressing SGR-GFP fusions, i.e. SGR1-GFP (S1-GFP; positive control), SGR2-GFP (S2-GFP), and negative control (GFP) plants were incubated in darkness for 2 d. Membrane-enriched fractions were used for pull-down experiments using  $\alpha$ -GFP antibody-conjugated agarose beads (GFP-IP). Co-precipitated proteins were detected by immunoblotting using respective antibodies. Input, immunoblot analysis of the fractions used for GFP-IP. These experiments were repeated more than twice with similar results.





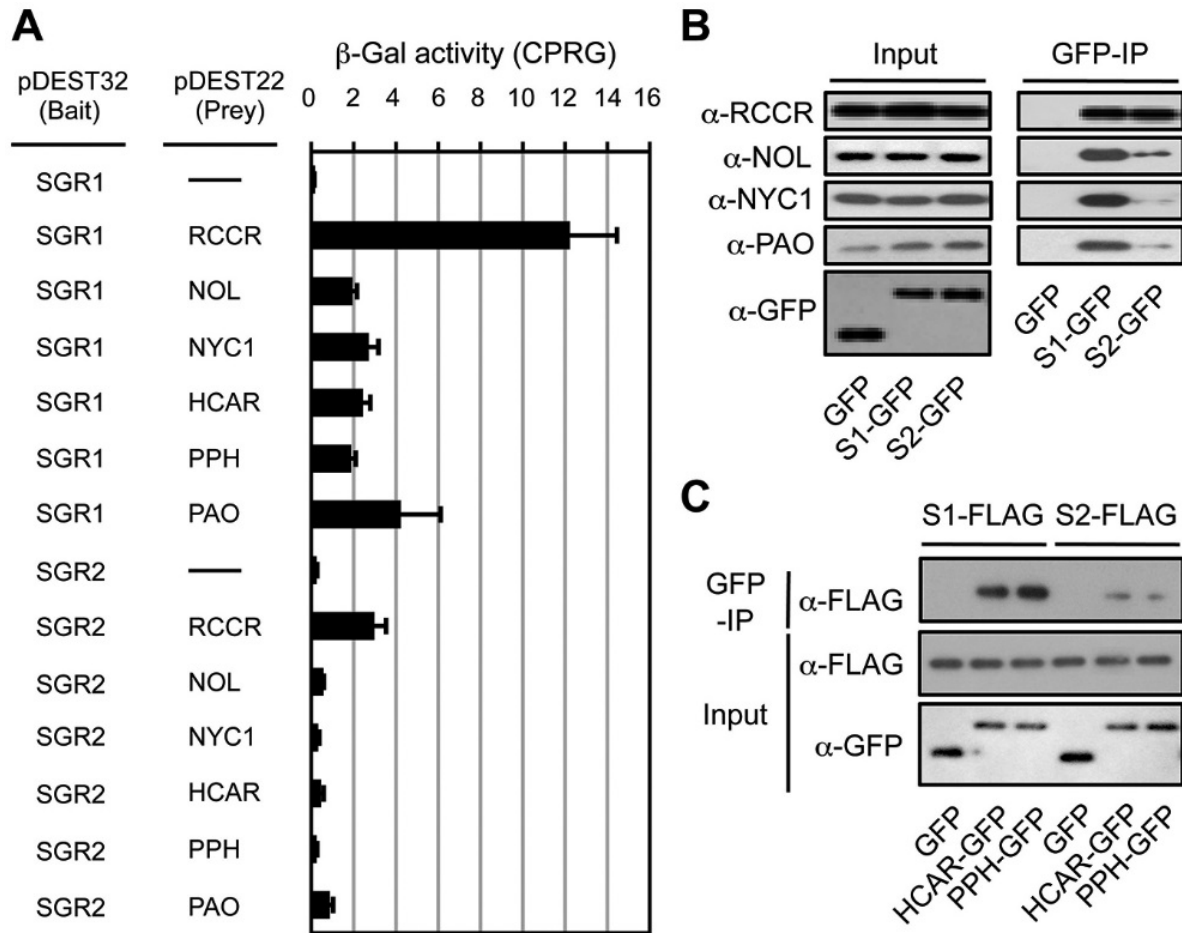


**Figure 7.** Physical Interactions of SGR1 and SGR2 with CCEs.

(A) Pairwise interactions of SGR1 and SGR2 with 6 CCEs in yeast two-hybrid assays. Relative β-galactosidase (β-Gal) activity was determined in liquid assays using chlorophenol red-β-D-galactosidase (CPRG) as substrate. Empty prey plasmids (-) were used as negative controls. Mean and SD values were obtained from five independent colonies.

(B) Co-immunoprecipitation of CCEs (RCCR, NOL, NYC1, and PAO) and SGRs in senescing chloroplasts. SGR1-GFP (S1-GFP), SGR2-GFP (S2-GFP), and GFP (negative control) transgenic plants grown for 3 weeks under LD conditions were transferred to darkness and sampled at 3 DDI. Membrane-enriched fractions were used for *in vivo* pull-down assays. GFP was immunoprecipitated (GFP-IP) with α-GFP-conjugated beads. RCCR, NOL, NYC1, and PAO in the input samples (left panel) and the pulled fractions (right panel) were detected using respective antibodies.

(C) Interactions between SGRs and PPH or HCAR by *in vitro* pull-down assays. Equal fresh weight of rosette leaves of 3-week-old transgenic *Arabidopsis* plants expressing FLAG-tagged SGRs and GFP-tagged HCAR or PPH (3 DDI) were co-homogenized. Membrane-enriched fractions were used for pull-down assays with α-GFP-conjugated beads (GFP-IP), followed by immunoblot analysis using α-FLAG. GFP transgenic plants were used as a negative control. These experiments were repeated more than twice with similar results.

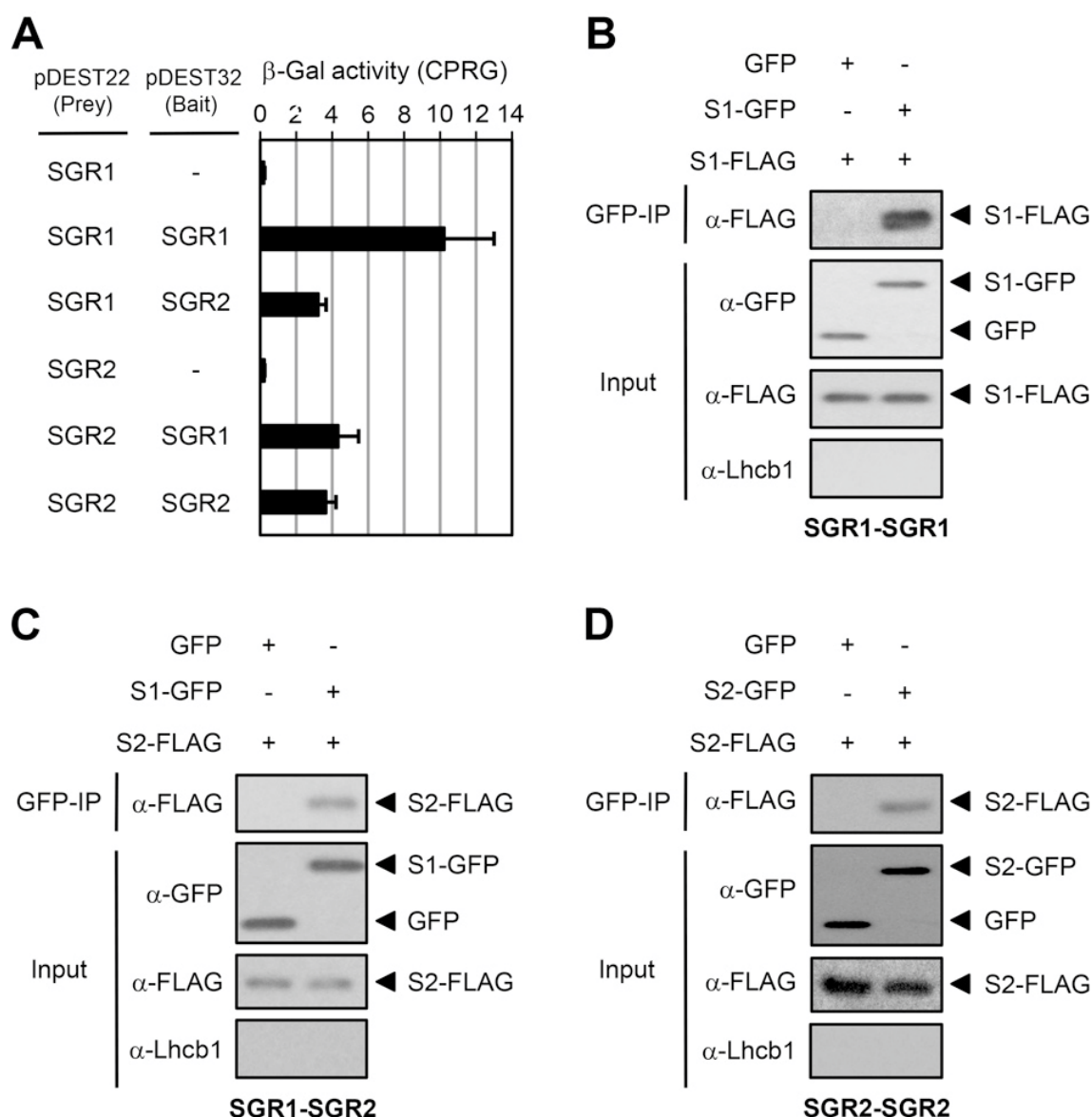


**Figure 8.** SGR1 and SGR2 Form Homo- or Heterodimers.

(A) Pairwise interactions between SGR1 and SGR2. Relative β-galactosidase (β-Gal) activity was determined in liquid assays using chlorophenol red-β-D-galactosidase (CPRG) as substrate. Empty bait plasmids (-) were used as negative controls. Means and SDs were obtained from five independent colonies.

(B-D) Interaction of SGR1 and SGR2 by *in vitro* pull-down assays. Equal fresh weight of 1-week-old etiolated seedlings of transgenic *Arabidopsis* lines expressing GFP-tagged SGR1 (S1-GFP) or SGR2 (S2-GFP) were co-homogenized with FLAG-tagged SGR1 (S1-FLAG) or SGR2 (S2-FLAG). Each homogenate was used for pull-down assays with α-GFP-conjugated beads (GFP-IP), followed by immunoblot analysis using α-FLAG. GFP transgenic plants were used as a negative control. The series of experiments was performed more than twice with similar results.